We are IntechOpen, the world's leading publisher of Open Access books Built by scientists, for scientists

4,800
Open access books available

122,000
International authors and editors

135M
Downloads

Our authors are among the

154
Countries delivered to

TOP 1%
most cited scientists

12.2%
Contributors from top 500 universities

CLARIVATE ANALYTICS BOOK CITATION INDEX INDEXED

WEB OF SCIENCE™

Selection of our books indexed in the Book Citation Index in Web of Science™ Core Collection (BKCI)

Interested in publishing with us?
Contact book.department@intechopen.com

Numbers displayed above are based on latest data collected.
For more information visit www.intechopen.com

Chapter 2

Small Scale Hydrogen Production from Metal-Metal Oxide Redox Cycles

Doki Yamaguchi, Liangguang Tang, Nick Burke,
Ken Chiang, Lucas Rye, Trevor Hadley and Seng Lim

Additional information is available at the end of the chapter

http://dx.doi.org/10.5772/50030

1. Introduction

The industrial production of hydrogen by reforming natural gas is well established. However, this process is energy intensive and process economics are adversely affected as scale is decreased. There are many situations where a smaller supply of hydrogen, sometimes in remote locations, is required. To this end, the steam-iron process, an originally coal-based process, has been re-considered as an alternative. Many recent investigations have shown that hydrogen (H_2) can be produced when methane (CH_4) is used as the feedstock under carefully controlled process conditions. The chemistry driving this chemical looping (CL) process involves the reduction of metal oxides by methane and the oxidation of lower oxidation state metal oxides with steam. This process utilises oxygen from oxide materials that are able to transfer oxygen and eliminates the need of purified oxygen for combustion. Such a system has the potential advantage of being less energy intensive than reforming processes and of being flexible enough for decentralised hydrogen production from stranded reserves of natural gas. This chapter first reviews the existing hydrogen production technologies then highlights the recent progress made on hydrogen production from small scale CL processes. The development of oxygen carrier materials will also be discussed. Finally, a preliminary economic appraisal of the CL process will be presented.

2. A brief overview on hydrogen production

Hydrogen can be produced from the reaction of feedstock including fossil fuels and biomass with water. Today, 96 % of hydrogen is derived from fossil fuels of which 48 %, 30 % and 18

% originates from natural gas, higher hydrocarbons and coal, respectively and the remaining 4 % comes from electrolysis. Fossil fuel based hydrogen production processes are mature technologies and are currently the most economic routes for large scale hydrogen production. Because coal, natural gas and biomass all contain carbon, carbon dioxide is inevitably produced as a by-product of the energy released. A pictorial overview of the available hydrogen production processes is given in Figure 1. The basics of two commercialised processes, namely steam methane reforming and partial oxidation, are considered in this section. A brief discussion on emerging hydrogen production technology will also be presented.

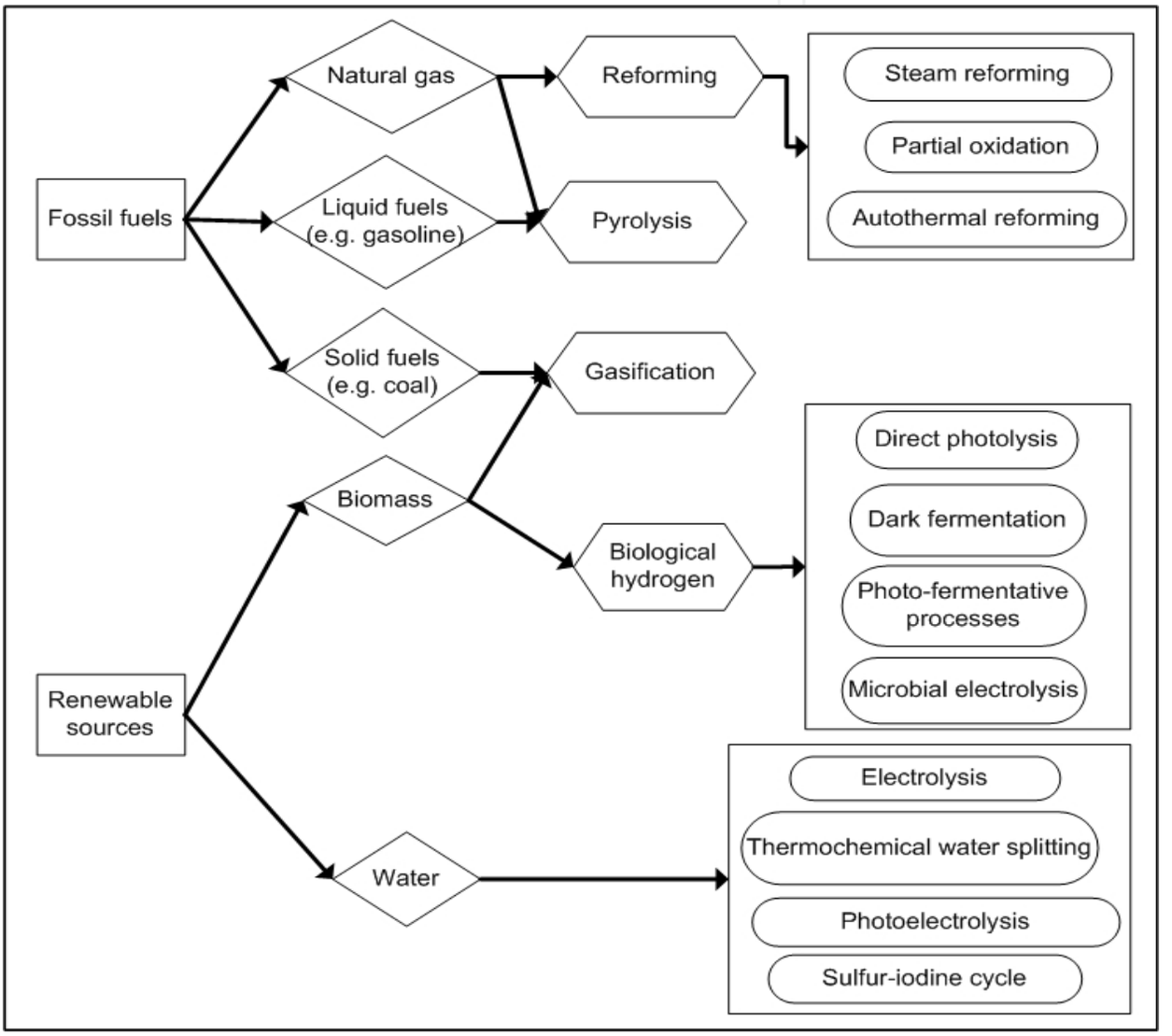

Figure 1. An overview of existing hydrogen production process from different sources.

2.1. Steam methane reforming

Steam reforming of methane (SMR) is one of the most developed and commercially used technologies. Compared to other fossil fuels, natural gas, which contains mostly methane, is

a cost effective feedstock for making hydrogen. This is because methane has a high hydrogen-to-carbon ratio, meaning the yield of hydrogen is higher. Today, almost 48 % of the world's hydrogen is produced from this technology [1]. In this process, hydrogen is produced according to the following two reactions:

$$CH_4 + H_2O \rightarrow CO + 3H_2 \Delta H° = 206 \text{ kJ/mol} \quad (1)$$

$$CO + H_2O \rightarrow CO_2 + H_2 \Delta H° = -41 \text{ kJ/mol} \quad (2)$$

In the SMR, the natural gas feedstock is first reformed in the presence of steam over a catalyst at elevated temperatures (700 – 925 °C) to produce a mixture of carbon monoxide and hydrogen (syngas) as shown in Equation 1. Then, the yield of hydrogen is further increased by reacting the carbon monoxide with make up steam via the water-gas shift reaction (WGS) as shown in Equation 2. Finally, hydrogen is separated and purified by processes such as pressure swing absorption, wet scrubbing or membrane separation. SMR is currently the most cost effective hydrogen production process which offers a minimum energy efficiency of 80 – 85 % in a large scale facility if residual steam is re-used [1]. Furthermore, the process is economically viable for large scale operation [2]. According to Pardor *et al.*[3], the price of hydrogen produced from SMR ranges from $5.97/GJ for a 25.4 million Nm^3/day plant to $7.46/GJ for a 1.34 million Nm^3/day plant. A figure of $11.22/GJ was estimated for hydrogen produced from a small facility (0.27 million Nm^3/day). However, the price of hydrogen varies with the price of natural gas feedstock. In general, the price of the natural gas feedstock accounts for 52 – 68 % and 40 % of the total cost for large and small SMR plants, respectively. It can be seen that decreasing the scale of operation would lead to an increase in cost of the hydrogen produced.

2.2. Partial oxidation

Hydrogen can also be produced from the partial oxidation (POX) of hydrocarbons over a catalyst at high temperatures (Equation 3).

$$CH_4 + 0.5O_2 \rightarrow CO + 2H_2 \Delta H° = -36 \text{ kJ/mol} \quad (3)$$

The reaction requires the use of high purity oxygen and is mildly exothermic. Similar to the SMR process, the yield and purity of hydrogen may be further increased by the WGS reaction and a subsequent purification process. The reported efficiency of POX is in the range of 66 – 76 % [1]. Mirabal [4] estimated the cost of hydrogen to be $12.43/GJ for a 2.83 million Nm^3/day plant, which is higher than that produced from SMR. However, based on the use of coke off-gas and residual oil (both having a price of lower than natural gas), Pardro *et al.*[3] estimated the price to be in the range of $6.94 – 9.83/GJ for large facilities (1.34 – 2.80 million Nm^3/day) and $10.73/GJ for a small facility (capacity is 0.27 million Nm^3/day). Similar to SMR, the economics appears more favourable for large scale operations.

2.3. Coal gasification

Gasification can be used to convert a varied range of solid fuels such as coal and biomass into syngas (Equation 4).

$$C(s) + H_2O \rightarrow CO + H_2 \Delta H^\circ = 131 \text{ kJ/mol} \quad (4)$$

Coal gasification is a mature process and is commercially available. Although the cost of the coal feedstock is generally much cheaper than natural gas, the price of hydrogen produced from coal gasification process is estimated to be $17.45/GJ. This is higher compared to SMR ($10.26/GJ) and POX ($12.43/GJ), and this is due to the higher capital investment required for coal gasification. Coal is an economically viable option for making hydrogen in very large centralised plants where the demand for hydrogen becomes large enough to support an associated large distribution network and establishment costs. It is therefore seen that coal gasification would become more competitive than SMR and POX as the price of natural gas increases [4]. Much of the engineering experience accumulated from coal fired power plant is directly useful for coal gasification.

2.4. Other novel routes for hydrogen production

Water splitting is one of the options for producing hydrogen and has received wide attention. The current reported energy efficiency is between 10 – 27 % and the cost of hydrogen is estimated to be 3-10 times of the hydrogen produced from the SMR process [5]. Biological routes for producing hydrogen are also being considered because of the renewable nature and the mild operating conditions of these processes. These alternative routes have yet to become economically competitive with technologies in practice such as SMR and POX that use fossil fuel feedstock.

3. Hydrogen production from cyclic redox processes

There is an ongoing demand for viable processes for producing hydrogen on a small scale for decentralised distribution. For this reason, there is currently much attention being paid to the development of cyclic redox processes or commonly referred as chemical looping (CL) processes for small scale hydrogen production. In addition to the compactness of the process, another advantage is the ability to produce a near sequestration-ready stream of carbon dioxide from the process. The operating concept behind these processes resembles the well-known steam-iron process and is illustrated in Figure 2a. Some widely reported variations and applications include chemical looping combustion (CLC) for power generation and, chemical looping hydrogen production (CLH2). The schematic diagrams representing these processes are shown in Figure 2b and Figure 2c. A typical chemical looping operation consists of a reduction and an oxidation steps. During the reduction, a metal oxide is used as the oxygen carrier to oxidise carbonaceous fuels (e.g. natural gas, coal or biomass) into carbon dioxide and steam. The reduction can be optimised such that syngas (a mixture of carbon monoxide and hydrogen) can be obtained. Subsequently, the partially or fully reduced metal

oxide is oxidised with air or steam to re-generate the original metal oxide and other oxidation products. When steam is used, water is split to produce hydrogen as the main product.

One of the fundamental parameters that determine the overall efficiency of many chemical looping processes is the effectiveness of the oxygen carriers. Therefore many research groups have focused on improving the activity and the stability of oxygen carrying materials. This section reports the latest developments of oxygen carrier materials for CL applications.

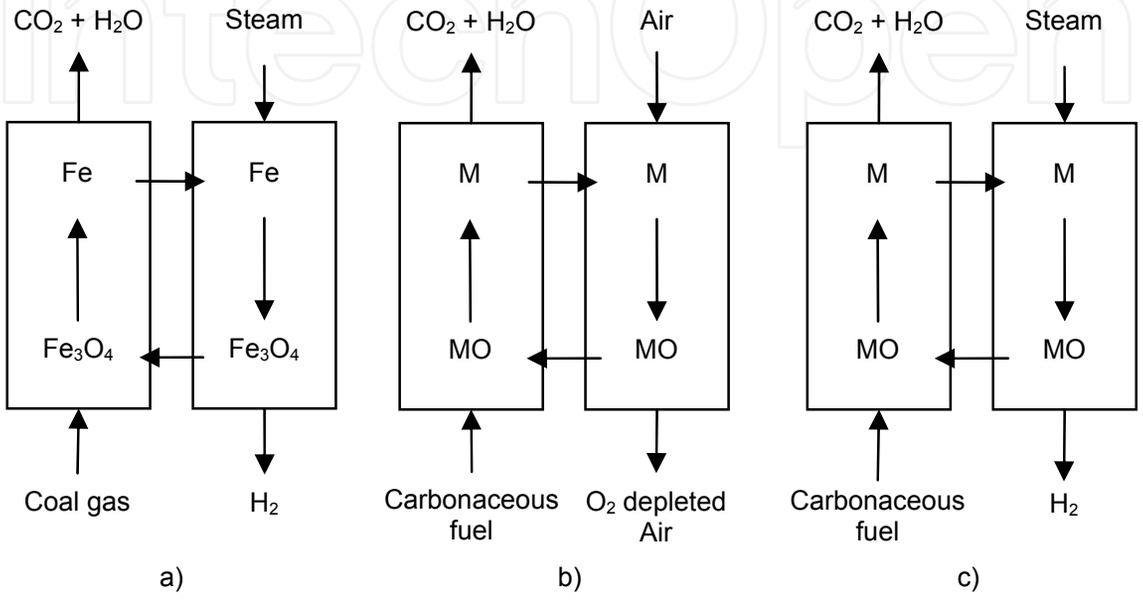

Figure 2. a) The traditional steam-iron process and chemical looping (CL) processes, b) CLC for power generation, and c) CLH2.

3.1. Thermodynamic constraints

The selection of an oxygen carrier requires comprehensive appraisal of the physiochemical properties of the material. Some properties include reaction kinetics, oxygen content, long-term recyclability and durability, attrition resistance, heat capacity, melting points, tendency to form coke, resistance to carbon deposition, cost and toxicity [6, 7]. Nevertheless, the most important requirement is the thermodynamic feasibility of oxygen transfer to and from these oxygen carriers. Figure 3 shows the changes in Gibbs free energy (ΔG) of some oxygen carriers commonly studied for CL applications. Some selected properties are provided in Table 1.

For the current topic, the oxygen carrier can be divided into two groups based on their ability to oxidise methane. The first group contains oxides that are capable of only partially oxidising methane into carbon monoxide and hydrogen. Some representative redox couples are ZnO/Zn, V_2O_5/V and CeO_2/Ce_2O_3 couples. The second group contains oxides that are able to support the complete oxidation of methane. NiO/Ni, CuO/Cu and Co_3O_4/Co are redox couples that fall into this category. In addition, the oxidations of these reduced oxides are favourable over a wide temperature range as indicated by the negative ΔG values in Figure 3. Therefore these three redox couples are often regarded as good candidates for CL applications.

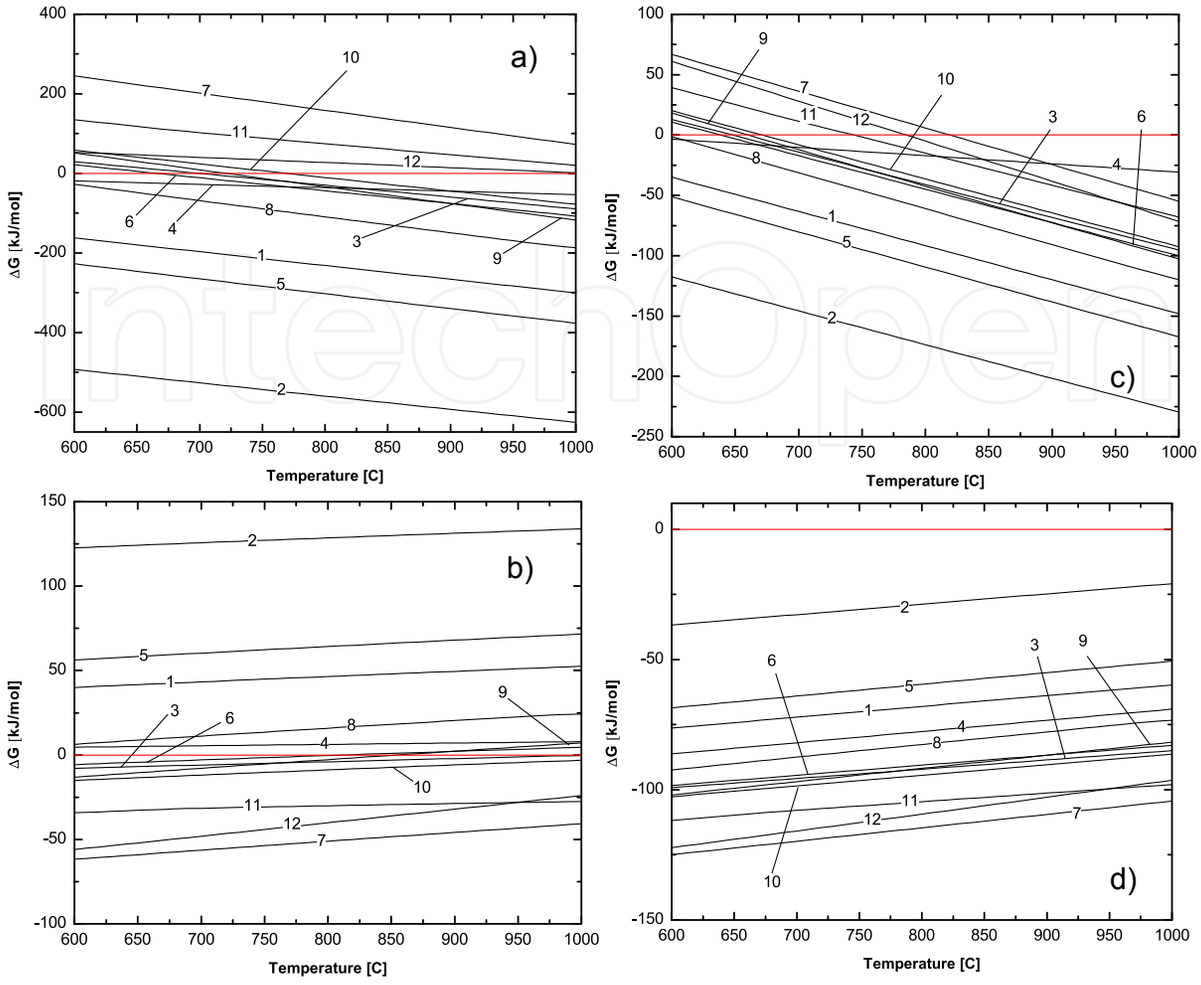

Figure 3. Variation of Gibbs free energy of reactions, a) CH_4 combustion ($CH_4 + 4/yM_xO_y \rightarrow CO_2 + 2H_2O + 4x/yM$) and b) CH_4 partial oxidation ($CH_4 + 1/yM_xO_y \rightarrow CO + 2H_2 + x/yM$), c) steam oxidation ($xM + yH_2O \rightarrow M_xO_y + yH_2$), and d) air oxidation ($xM + y/2O_2 \rightarrow M_xO_y$). See Table 1 for the legendsused.

Number	Redox couple	Melting point [°C]	Oxygen transport capacity [kg/kg-metal]	Price [USD/t]
1	NiO/Ni	1955/1455	0.27	21,800
2	CuO/Cu	1326/1084	0.25	7,680
3	Fe_3O_4/Fe	1597/1538	0.38	100
4	MnO_2/Mn	535/1267	0.58	1,500
5	Co_3O_4/Co	895/1495	0.36	39,700
6	WO_3/W	1472/3407	0.26	27,000
7	ZnO/Zn	1975/420	0.24	2,250
8	SnO/Sn	1080/232	0.13	21,000
9	In_2O_3/In	1913/157	0.21	565,000
10	MoO_2/Mo	1100/2623	0.33	34,900
11	V_2O_5/V	670/1910	0.78	25,600
12	CeO_2/Ce_2O_3	2400/2230	0.06	24,611

Table 1. Selected properties of oxygen carriers.

Compared to oxidation using molecular oxygen, the ΔG shifts to higher values when steam is used as the oxidising agent. As a result, it is not thermodynamically feasible to produce hydrogen by reacting steam with metallic Ni, Cu or Co.MnO_2/Mn and SnO/Sn couples are also not reactive when they are brought into contact with steam. ZnO/Zn and V_2O_5/V couples react with steam to produce hydrogen, however, their melting points in either the oxide or the metallic form are too low for CL applications in general. Despite the moderate ΔG values associated with Fe_3O_4/Fe, WO_3/W and CeO_2/Ce_2O_3 redox couples, the reported redox kinetics and thermo-mechanical strength have made them appealing candidates for CL processes. The Fe_3O_4/Fe couple also possesses a relatively high oxygen content, and is widely available, non-toxic and less costly. When iron oxide is used, it is only possible to oxidise the reduced state to magnetite (Fe_3O_4) due to thermodynamic limitations.

3.2. Common feedstocks for producing hydrogen

A number of studies have employed non-gaseous fuels including coal [8-13], biomass [14-17] and pyrolysis oil [18, 19]. In a syngas chemical looping (SCL) process, the fuel is first converted into syngas in a separate gasification unit. The syngas generated is then used in the reduction cycle and steam is used to regenerate the oxide and to produce hydrogen. An additional air oxidation cycle may be required to regenerate the oxygen carrier. The SCL process generally has lower efficiency for conversion, owing to the low conversions in the syngas generation step and the steam oxidation step [8]. Li et al. [9] examined the cyclic performance of a Fe-based oxygen carrier at 830 °C when a simulated syngas was used. They showed that the syngas was completely converted in the reduction half cycle giving an oxygen carrier conversion of 94.6 %. For the steam half cycle, the reduced oxygen carrier was oxidised into Fe_3O_4 producing a stream of 99.8 % pure hydrogen. In a separate study, the same group also demonstrated the feasibility of using a moving bed reactor at 900 °C for the same reaction[10]. A syngas conversion in excess of 99.5% and an oxygen carrier conversion of 50 % were recorded. A process simulation conducted by Gupta et al. [8]confirmed that the maximum efficiency for the SCL process could reach 74.2 % for hydrogen production which is comparable to or more effective than steam reforming (65-75 %), partial oxidation (50 %) and gasification (43-47 %). Considering the complexity of the SCL, it is clear that footprint of the process would be large because of the large number of unit operations involved in its design.

When coal is used as the feedstock, the solid fuel can be used to reduce oxygen carriers directly. This process is often referred as the coal direct chemical looping (CDCL) process because a gasification unit, as well as air separation and gas cleaning units, is not required [12]. The CDCL process is reported to be significantly more efficient than the SCL process for hydrogen production [6, 13].Yang et al. [11] investigated the CDCL process using a lignite-derived char in a fluidised bed reactor. The complete gasification of the char achieved a maximum carbon dioxide concentration of 90% in the presence of a K_2CO_3 catalyst. A high oxygen carrier-to-char ratio improved the complete gasification to carbon dioxide but this also led to lower hydrogen yields as a result of low conversions of the oxygen carrier. Under the optimum condition, the hydrogen production efficiency was

reported to be 50.2 % at an oxygen carrier conversion of 70.2 %. The use of counter-current moving bed reactor was found to improve oxygen carrier conversion, and achieved (due to the significantly low mass required) a char conversion of > 90 % and an overall carbon dioxide capturing efficiency of > 95 %[6].

Biomass has found limited applications for SCL processes. This is because of the high water content generally associated with biomass feedstocks. Sime et al. [14] investigated the use of gases derived from woody biomass gases for SCL and reported that such process was less efficient and more costly than conventional gasification processes for producing hydrogen. Li et al. [16] pointed out that it is critical to reduce the moisture content in the biomass feedstock to less than 5 %in order to achieve a conversion of 56.6 % in gasification. Similar to other solid feedstocks, unreacted biomass must be separated before the oxygen carrier is circulated to the steam reactor. Otherwise, the unreacted biomass could be gasified and lower the purity of the hydrogen produced.

Natural gas is an efficient feedstock for CL processes since it is fed to the process in gaseous form. This minimises the need of solid handling and improves mass transfer processes [20]. Cormos (2011) recently assessed and compared hydrogen production from a natural gas CL process and a coal/lignite based SCL [21]. It was concluded that when natural gas was used to produce hydrogen, the recorded efficiency was 78.1 %. This value was higher compared to the values of 65.7 % and 63.3 % recorded for the coal- or lignite-based SCL processes, respectively. In addition, the separation and capturing of CO_2 were said to be more effective when natural gas was used. Another clear advantage of using natural gas as the feedstock is that no additional up-stream unit operations are required for producing syngas.

3.3. Oxygen carriers for cyclic redox processes

As mentioned previously, redox kinetics and thermal stability are the two main issues associated with the use of oxide-based oxygen carriers for CL processes. In order to improve their performance, support and/or promoting materials to assist in material stabilisation are often added to improve the performance of the metal oxide. A comprehensive list of oxygen carriers developed for various CL applications in the last decade can be found in an excellent review published by Adanez et al. [7]. This section highlights some recent studies on developing novel oxygen carriers.

3.3.1. Effects of metal addition to oxide carriers

Otsuka et al. [22, 23] investigated the effects of 26 different metal dopants on iron oxide. It was found that some metal dopants were more effective in preventing the iron oxide from sintering and some were more effective in facilitating the splitting of water. Among these 26 metals, Mo and Cr were found to improve the thermal stability of iron oxide in the cyclic process. The improved redox stability after the introduction of Mo metal (5 mol%) was also reported by Wang et al. [24], and Liu and Wang [25]. Despite the fact that Cr addition could improve the sintering resistance of iron oxide, temperature programmed analysis revealed that a temperature of ca. 500 °C is required to split water when compared to a temperature

of 420 °C as required by iron oxide modified with Mo [22]. In addition, no oxidation of methane was observed when the temperature was lower than 700 °C [26]. It was proposed that the main role of Cr and Mo dopants was to partially transform the iron oxide into the ferrite structure ($M_xFe_{3-x}O_4$, M = Mo and Cr) [22, 26] and therefore inhabited the agglomeration of neighbouring particles.

Some metals including Ru, Rh, Pd, Ag, Ir and Pt have been shown to improve reaction kinetics by facilitating the dissociation of hydrogen, methane and water. Otsuka et al. [22] reported that the improvement on splitting of water into hydrogen by metal in a CLprocess increased in the order of Rh > Ir > Ag > Pd > Ru. Ryu et al. [27] also found that Rh was more effective than Pb, Pt and Ru in enhancing the hydrogen production step in a chemical looping process. The role of Rh was to decrease the onset temperature for the water splitting reaction. A XANES/EXAFS study on Rh-Cr-added iron oxide revealed that Rh was also able to form Rh-Fe alloy upon reductions[26]. However, Rh segregated in the alloy structure when it contacted steam and thus accelerated the sintering of iron oxide. This led to the observed deterioration in redox activity after repeated redox operation. Although Ni- and Cu-ferrites also exhibited an enhancing effect on redox kinetics, Ni and Cu were shown not to be effective in improving sintering resistance [28, 29].

The addition of a second and a third metal have been shown to further improve the redox activity [22, 24-27, 30, 31]. Common choices of metal combinations often consisted of a first metal such as Rh, Pt, Ni and Cu which is thought to catalytically activates the reducing gas (e.g. hydrogen, carbon monoxide or methane), and a second metal such as Mo and Cr which exhibits a structural stabilising effect. Otsuka et al [22] examined the addition of Rh and Mo to iron oxide for the chemical storage of hydrogen and observed an enhancement in reaction kinetics and a reduction in reaction temperature for hydrogen formation. Most importantly, the Mo provided good stabilising effect and largely mitigated the sintering of the oxygen carrier. The effect of bimetal addition on iron oxide was also investigated under methane oxidation at a temperature range of 200 – 800 °C by Takenaka et al. [30]. The methane conversion was found to increase by adding a second metal and the performance increased in the order of Rh-Cr > Ir-Cr > Pt-Cr > Ni-Cr > Pd-Cr > Cu-Cr = Co-Cr. Other research groups also reported similar findings [24, 25, 27, 31]. Despite the improvement in reactivity and thermal stability, most of the bimetallic modified oxygen carriers produce carbon upon methane oxidation. The production of carbon usually leads to a rapid deterioration of the oxygen carrier and is the source of carbon oxides (CO_x) contamination.

3.3.2. Supported oxygen carriers

Another approach to improve the thermal stability of oxygen carriers is to introduce inert support materials such as Al_2O_3, SiO_2, TiO_2 and ZrO_2. Adanez et al. [32] assessed the reactivity of 240 different types of oxygen carriers composed of Cu, Fe, Mn or Ni supported on SiO_2, TiO_2, ZrO_2, Al_2O_3 or sepiolite ($Mg_4Si_6O_{15}(OH)_2 \cdot 6H_2O$) over a temperature range of 950 – 1300 °C. The best Fe-based oxygen carriers were those supported on Al_2O_3 or ZrO_2. It was also found that the formation of aluminate ($NiAl_2O_4$ and $CoAl_2O_4$) lowered the oxygen transport capacity and hence reduced the redox activity [33]. SiO_2 was found to be the most

suitable support for Cu-based oxygen carrier because it remained inert at high temperatures and did not form Cu-SiO_2 composites. However, Fe-based oxygen carriers showed a strong tendency to form unreactive iron silicates with SiO_2[34]. ZrO_2 and TiO_2 were suggested as the best supports for Mn- and Ni-based oxygen carriers, respectively. In terms of the cyclic redox activity, however, TiO_2 supported Ni-based oxygen carriers showed lower reactivities, compared to Ni supported on Al_2O_3. This is because NiO is more prone to react with TiO_2 and form $NiTiO_3$ which is known to be less reducible than NiO. It also exhibits a high carbon formation tendency. Therefore, Al_2O_3 supported Ni-based oxides were considered to be the most promising oxygen carrier for a large scale CLC applications.

Some metal doped iron oxide oxygen carriers were also supported on ZrO_2 for CL processes [29, 35-37]. Kodama et al. [35, 36] showed improved thermal resistance for the Ni- and Co-ferrites when ZrO_2 support was introduced. The reported methane conversion and carbon monoxide selectivity by using $Ni_{0.39}Fe_{2.61}O_2$ (33 wt%)/ZrO_2 were 46-58% and 44-48%, respectively. However, since Fe and Ni are excellent catalysts for methane decomposition, the material was severely deactivated by coke and the subsequent carbide species formed. Because Cu has lower activity for methane decomposition, $CuFe_2O_4$ was used to produce syngas from methane [29]. The results showed that no CO_x was formed during the operation. The same group also found beneficial effects of ZrO_2 and CeO_2 supports for $CuFe_2O_4$ (20 wt%) [38]. Compared to the methane conversion obtained for $CuFe_2O_4$ (34–56 %), the methane conversions achieved by $CuFe_2O_4/CeO_2$ and $CuFe_2O_4/ZrO_2$ were 89-92 % and 74-83 %, respectively. From these results, CeO_2 was found to be more active in promoting methane oxidation while ZrO_2 was considered to be a more effective stabiliser against thermal sintering. Since CeO_2 is known to be able to oxidise soot through lattice oxygen transfer [39, 40], it is thought that this property could help to minimise carbon formation when $CuFe_2O_4/CeO_2$ is used. Cha et al. [37] also confirmed that CeO_2 modified $CuFe_2O_4/ZrO_2$ was a more effective oxygen carrier than Ni-modified $CuFe_2O_4/ZrO_2$ for chemical looping syngas and hydrogen productions.

A recent study conducted by Yamaguchi et al. [41] also demonstrated the improved performance of CeO_2/ZrO_2 modified $Fe_2O_3$for producing hydrogen from methane-steam cycles. Some results obtained from temperature programmed analysis and isothermal reduction are shown in Figure 4 and are summarised in Table 2. Figure 4a shows that CeO_2 and ZrO_2 altered the redox properties of Fe_2O_3 with the most significant enhancement observed for the reducibility at low temperatures (< 600 °C) (see Table 2). The isothermal reduction analysis (Figure4b) further confirmed the accelerated reduction kinetics after the introduction of CeO_2 and ZrO_2. The observed overall enhancement was derived from the combined effects of CeO_2 and ZrO_2. CeO_2 improved the reducibility of Fe_2O_3 while ZrO_2 provided thermal stability and helped to suppress the reduction of FeO to metallic Fe. The latter was supported by the incomplete reduction of $Fe_{15}Ce_{10}Zr_{75}$ and $Fe_{40}Zr_{60}$ (Table2).Similar observations were also reported when WO_3 was modified with CeO_2 and ZrO_2[42]. The synergic effect provided by CeO_2 and ZrO_2 effectively defined the redox window of the oxygen carriers. An immediate consequence is the minimisation of carbon and carbide formation during repeated redox cycles. This can be demonstrated by the fact that CO_x free hydrogen was produced by using CeO_2-ZrO_2 modified WO_3 in a methane-

steam CL process [42]. The addition of a small amount of Mo or Cr could further improve the thermal stability of this type of oxygen carrier. Galvita et al. [43] showed the addition of 2 wt% of Mo to $Fe_2O_3/Ce_{0.5}Zr_{0.5}O_2$ could maintain a stable level of hydrogen production over 100 cycles in a cyclic water-gas shift process. In this reaction, the main role of Mo is to improve the dispersion of Fe-Mo oxide material and minimise the migration of material across the boundary of adjacent particles [44].

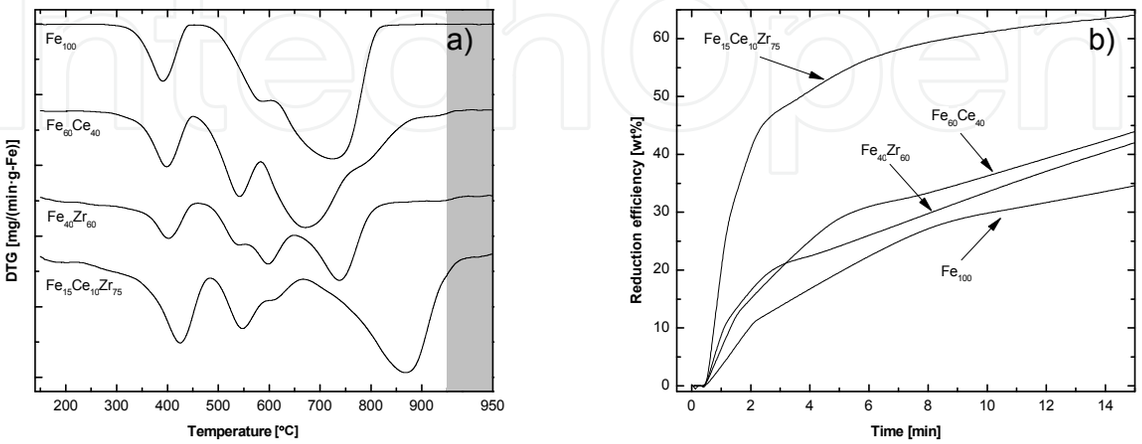

Figure 4. Effect of CeO_2 and/or ZrO_2 addition on Fe_2O_3 reducibility during a) temperature programmed and b) isothermal reduction with H_2[41].

Oxygen carrier	Oxygen removal[1] [mg-O/g-Fe]	Overall reduction efficiency[2] [wt%]	H_2 yield [μmol/g-Fe]	H_2 purity [%]
Fe_{100}	125	98.1	15	11.5
$Fe_{60}Ce_{40}$	169	97.1	368	49.1
$Fe_{40}Zr_{60}$	153	66.7	88	17.4
$Fe_{15}Ce_{10}Zr_{75}$	255	77.2	6283	97.5

Table 2. A summary of oxides used in methane-steam redox cycle [41]. [1]The oxygen removal represents a cumulative weight reduction at temperatures < 600 °C during the TPR analysis (Figure4a). [2]The overall reduction efficiency represents a final reduction efficiency obtained during isothermal reduction analysis at 750 °C for 240 min.

3.3.3. Naturally occurring oxide materials

Recently, many naturally occurring minerals and ashy waste produced from industry have been considered for use as oxygen carriers. These materials include natural ilmenite (Fe and Ti mixed oxide often denoted as $FeTiO_3$), iron ore, manganese ore and oxide scales. An advantage of using these materials is the low cost compared to many synthetic oxygen carriers. In addition, naturally occurring oxides usually contain Si, Al, Mg, and many other metals which have been shown to modify the physiochemical properties of the materials to various degrees. Leion et al. [45] investigated the feasibility of using ilmenite, iron ores, oxide scales from steel industry and manganese ores as oxygen carriers in a fluidised bed reactor. They concluded that many Fe based oxides, particularly ilmenite, were suitable for CLC

application. However, the Mn-based oxides showed poor mechanical stability and fluidising properties, and were determined to be non-ideal candidates for this application. In a separate study, Leion et al. [46] also proved the feasibility of using ilmenite to completely capture carbon dioxide upon its reaction with syngas and reported a moderate conversion when methane is used. Adanez et al. [47] observed increases in ilmenite, and syngas and methane conversions with increasing the time on stream and the number of redox cycles. Another important finding was the enhanced activation of ilmenite when the raw ilmenite material was subjected to an oxidation pre-treatment. The authors also found the redox properties of ilmenite changed with the temperature of oxidative pre-treatment. However, the positive effect only became apparent when the ilmenite was first oxidised to pseudobrookie (Fe_2TiO_5) which is usually formed above 1000 °C.

Pre-oxidation temperature [°C]	Major crystalline phases[1]	Oxygen transfer capacity [wt%]
Raw	$FeTiO_3$, TiO_2	1.1
800	Fe_2O_3, TiO_2	1.0
1000	Fe_2TiO_5, TiO_2	1.8

Table 3. Oxygen transfer capacity and major phase of various ilmenite samples before and after pre-oxidation. [1] Phases were identified by XRD analysis

Leion et al. [46] also reported that an ilmenite sample remained active with minimum carbon formation after a continuous operation for three days at 975 °C. Furthermore, natural ilmenite is known to react just as well with petroleum coke, syngas and methane as synthetically prepared $Fe_2O_3/MgAl_2O_4$[48]. Lorente et al. [49] reported a better hydrogen storage capacity and redox stability when iron ore samples was used instead of pure Fe_2O_3. The improvement in the overall redox performance was due to the presence of impurities including SiO_2, Al_2O_3, MgO and CaO. Among these impurities, Al_2O_3 and SiO_2 are considered to be good stabilisers against sintering, while CaO and MgO are able to facilitate kinetics of water splitting.

3.4. Deactivation of oxygen carriers

The life time of the oxygen carrier is a critical factor in determining the efficiency and viability of CL processes. In general, the efficacies of oxygen carriers decrease over time because of material alternation by sintering and/or coking.

Generally, for the CLH2 application, a relatively high temperature is required for driving the reduction reaction in order to achieve satisfactory conversion and kinetics. As a result, the high temperature environment irreversibly alters the structure and the morphology of oxygen carriers, and lowers the activity during the cyclic operation. The sintering process starts as two spherical particles adhere to one another. The process involves the diffusion of metal cations between neighbouring spheres. Figure 5 shows the SEM images of a pure Fe_2O_3 sample and the same material recovered after six methane-steam redox cycles performed at

750 °C. Severe sintering is clearly evident. The heat generated from the redox reactions could accelerate the rate of sintering. When oxygen carriers sinter and agglomerate inside a fluidised bed reactor, bed defluidisation may occur. The change in solid circulation and the subsequent occurrence of gas by-pass would significantly lower the gas-solid contact and hence the overall conversion efficiency.

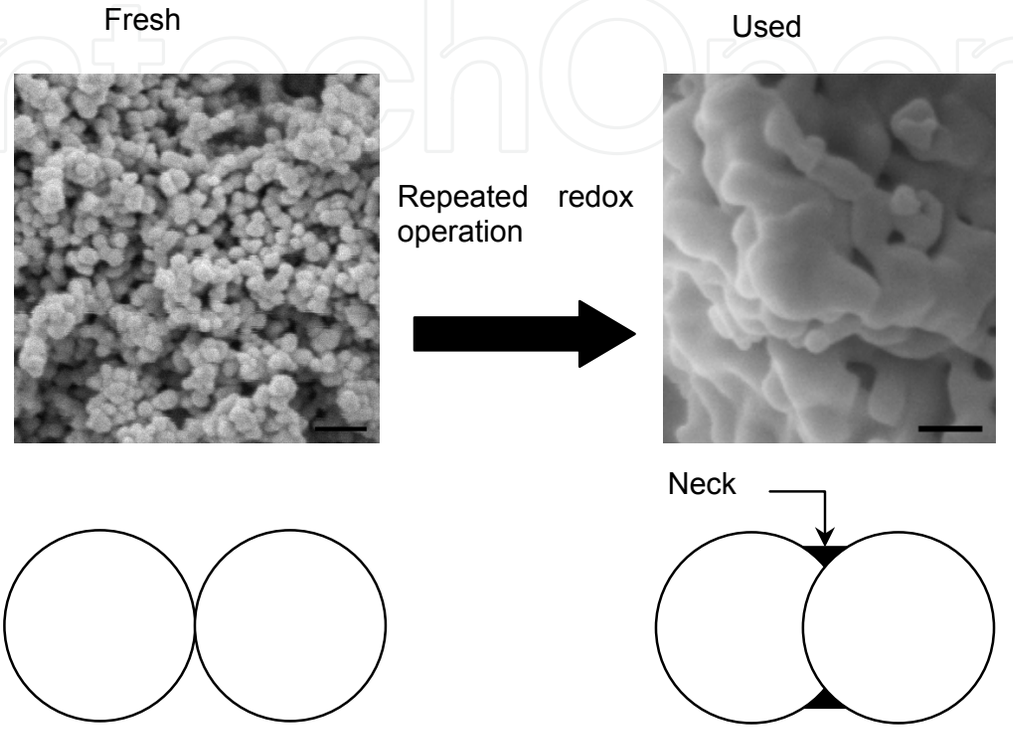

Figure 5. SEM images of Fe_2O_3 sample before and after six methane-steam redox cycles at 750 °Cand representative schematics of neck growth between two particles[41].

One of the approaches to minimise material sintering is to inhibit the diffusion in the solid particle. The complete reduction of the oxygen carrier to the corresponding zero valent metal is also a main cause of sintering since most metals agglomerates easily under elevated temperature conditions. Fukase and Suzuka [50] reported that the formation and accumulation of FeO during CL operation was mainly responsible for deactivation when iron oxide was used as the oxygen carrier. They also pointed out the importance of balancing the stoichiometry of reduction and oxidation of iron oxide and to avoid the formation of FeO by controlling reduction and oxidation temperatures. It is also important that the reduced iron species were completely oxidised to Fe_3O_4 phase. This mitigates the crystallite growth of the iron oxide and effectively prevents it from any structural changes.

Carbon is a common by-product of the CL process when a carbonaceous fuel is used as the feedstocks. Two possible routes for carbon formation are the decomposition of methane (Eq. 5) and the Boudouard reaction (Eq. 6). Methane decomposition is an endothermic reaction, and it is thermodynamically favourable at a high temperature, while the Boudourard reaction is favourable at a low temperature. These reactions could become significant in the presence of catalysts. Upon reduction, many metal oxides such as NiO, CuO and Fe_2O_3

could give rise to active metal centres which are able to rapidly produce carbon on the oxygen carrier surfaces. Once the solid carbon is formed, it will be carried over to the subsequent oxidation cycle where it is gasified to produce CO_x. When this happens, the purity of the hydrogen produced will be inevitably lowered.

$$CH_4 \rightarrow C + 2H_2 \quad \Delta H^\circ = 74.6 \text{ kJ/mol} \tag{5}$$

$$2CO \rightarrow C + CO_2 \quad \Delta H^\circ = -172.4 \text{ kJ/mol} \tag{6}$$

In general, as the oxygen ratio in the system decreases, there is a higher tendency towards carbon formation. The oxygen ratio is defined as the actual amount of oxygen contained in the metal oxide to the stoichiometric amount of oxygen required for complete oxidation of the fuel. It is also clear that carbon formation becomes more favourable as the oxygen in the oxygen carrier is depleted through the reaction with fuel. Cho et al. [51] reported that when more than 80 % of the available oxygen in the Ni-based oxygen carrier was consumed, the rate of carbon formation increased rapidly. This was accompanied by a drastic decrease in the fuel conversion because of the decreasing oxygen content available for oxidation. Galvita and Sundmacher [43] reported that a maximum Fe reduction of 60 % largely minimised carbon formation and a high purity hydrogen stream (< 20 ppm CO) could be obtained.

4. Process economics

In view of the lack of information on the cost of hydrogen produced from the CL process, the preliminary economic analysis and greenhouse gas footprint (GHG equivalent emissions in terms of carbon dioxide) of a methane-steam redox process will be provided in this section. A simple design for hydrogen production via a two-reactor layout was first obtained by considering the mass and energy balances as well as the overall pressure balance in order to establish a circulation of solids between the two reactors. The means of exchanging heat (direct, indirect, counter-current, available surface area, approach temperatures etc) has been considered, but has not been addressed further in this study. The pressure balance was affected by variables including the physical properties of the solid and gas, fluid velocity, solids recirculation rate as well as the geometry of the system. The pressure balance was solved using a one-dimensional model[52]. The basis of the design was a hydrogen production rate of 49 kg/h (or 547 Nm^3/h). This process considered the use of iron oxide as the oxygen carrier. Because the reduction of the iron oxide was much slower than its oxidation, a bubbling fluidised bed was chosen for the fuel reactor and a riser for the steam reactor. A particle size and density of the iron oxide particles were assumed to be 160μm and 5850kg/m^3, respectively. Other assumptions made for the operation are listed in Table 4. A high solids (i.e. the iron oxide) flow rate was required through the riser in order to meet the mass balance. This resulted in a high pressure drop across the riser, which was reduced by increasing the excess steam used for oxidation of the reduced iron oxide in the riser (at constant superficial gas velocity). The resultant mass balance is given inFigure6 and the CLH2 design is presented in Figure 5.

	Steam Reactor (riser)	Downcomer	Fuel Reactor (bubbling fluidised bed)	Loop Seal to Steam Reactor
Superficial gas velocity [m/s]	6.0	0.1	0.15	0.1
Temperature [°C]	750	700	750	700
Feed gas	Steam	Steam	Natural Gas	Steam
Feed gas temperature [°C]	240	240	500	240
Feed gas pressure [bar]	5	5	5	5
Conversion	100% FeO to Fe_3O_4	None	20% F_3O_4 to FeO 100% conversion of NG	None
Residence time required			1 minute	

Table 4. Assumptions used in the design of a CLH2process.

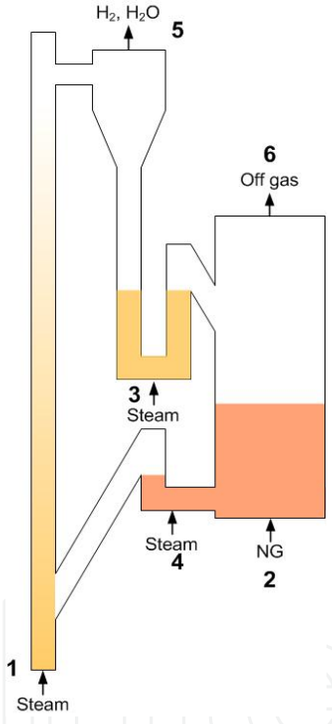

	1	2	3	4	5	6
Solids			**98166**	**97776**		
FeO			0.0%	5.4%		
Fe_3O_4			28.8%	23.1%		
Support			71.2%	71.5%		
Gas	**1320**	**99**	**108**	**108**	**1145**	**489**
O_2						
N_2						
H_2O	100.0%		100.0%	100.0%	95.7%	44.3%
H_2					4.3%	
CH_4		89.3%				0.0%
C_2H_6		8.5%				0.0%
C_3H_8		2.2%				0.0%
CO_2						55.7%

Figure 6. A schematic of CLH2processand the mass balance used for hydrogen production. Flow rates are represented in kg/hr and compositions in mass percentage.

The process flow diagram including the major peripheral equipment is shown in Figure 7. The heat from the exothermic reaction in the riser is used to raise superheated steam at 20 bar and 400 °C. This is used to generate electricity, with the steam let down to 5 bar and 240 °C. 25% of the steam is used as feed to the steam reactor and to fluidise the two loop seals. The water vapour content in the hydrogen product stream is due to the excess steam fed to the riser as well as from steam used to fluidise the loop seals. This is condensed out and returned with the water from the steam turbine to the boiler, in order to reduce the fresh water requirement. The heating required for the endothermic reaction in the fuel reactor is reduced

		Steam reactor	Steam down-comer	Fuel reactor	Units
Gas flow	Entering	957	16	159	Nm^3/h
	Exiting	457	14	137	Nm^3/h
Superficial gas velocity		6.0	0.1	0.15	m/s
G_s	Entering	346	346	51	$kg/m^2 \cdot s$
Internal diameter		0.32	0.32	0.83	m
Temperature		750	700	750	°C
Pressure	Bottom	113	98	107	kPa,g
	Top	102.45	179.31	179.31	kPa,g
Height	Total internal	15	-	3.9	m
	Gas exit (from top of riser)	0.8	-	-	m
	Downcomer (not including cyclone)	-	7	-	m
	Bubbling bed /loop seal	-	0.7	1.1	m
Height relative to datum					
	Bottom	0.0	5.1	1.9	m
	Loop seal entrance to riser	1.2	-	-	m
Solids void age (ε)		0.88	0.47	0.53	

Table 5. Reactor configuration for CLH2process.

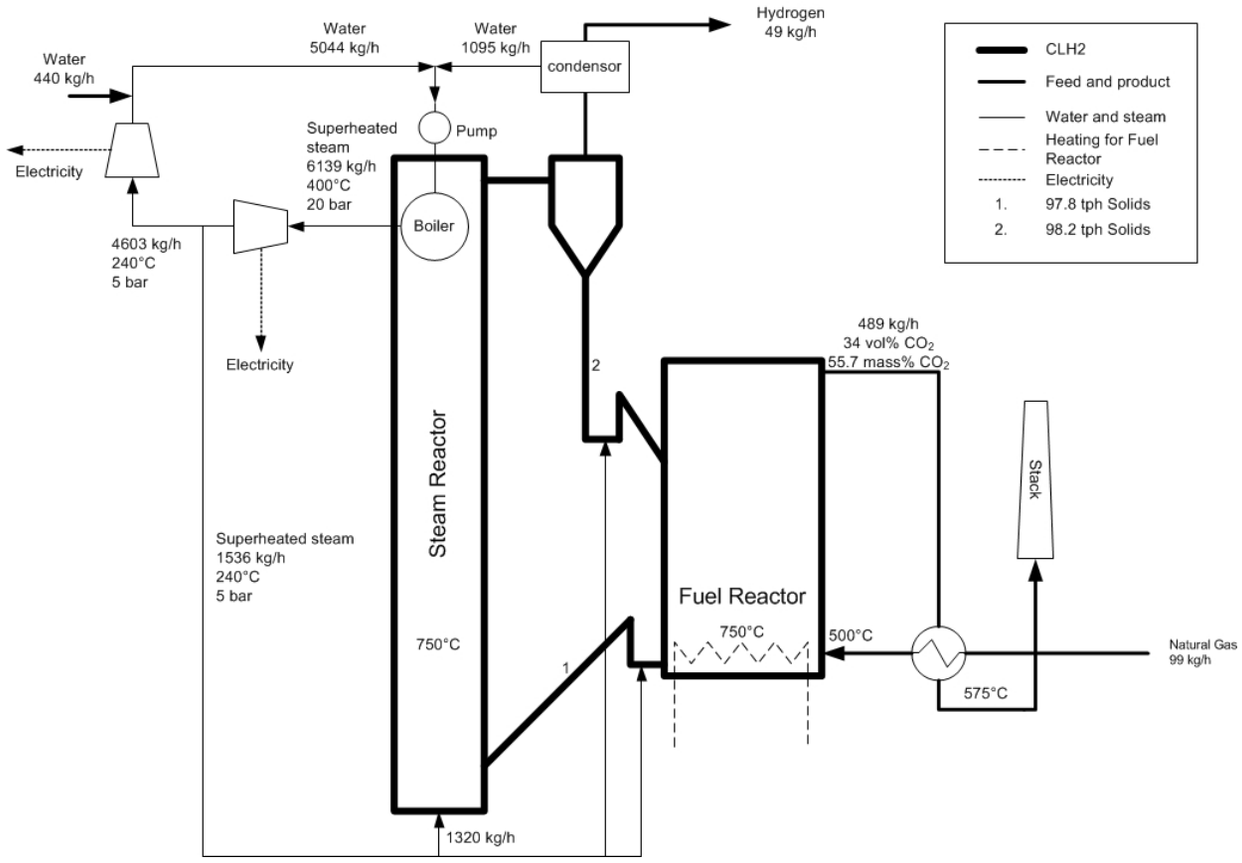

Figure 7. Proposed flow diagram of CLH2 process, showing peripheral equipment.

by pre-heating the natural gas using the waste heat from the off gas from the fuel reactor. For the current heat balance purpose it is assumed that there are different ways of supplying this remaining heat. One of the possible ways of supplying direct heat is by including a third combustion loop operated at higher temperature, which is outside the scope of this study.

The greenhouse gas emissions associated with the production of a unit of hydrogen were calculated using lifecycle assessment (LCA) techniques. Principally, LCA is a technique used to assess the environmental impacts of all stages associated with the production, use and disposal of a product or delivery of a service (product life from cradle to grave). In the case of a fossil fuel for example, this includes not only the combustion emissions associated with the fuel's use, but also includes pre-combustion or upstream emissions resulting from the extraction, production, transportation, processing, conversion and distribution of the fuel. The international standards contained in the ISO 14040 series [53] provide a basic framework in which to undertake LCA. A more general introduction to LCA may be found in Horne et al. [54]and Weidema et al. [55].I n this study, all fuel production and feedstock supply processes, as specified in Figure 7, were included in the LCA. The analysis is therefore limited to processes upstream of the refinery gate and thus does not include the delivery and combustion of hydrogen. Emission results are reported using the concept of a global warming potential (GWP), which enables different greenhouse gases to be compared and expressed using an equivalent carbon dioxide (gCO_2e) value. Data used for the analysis are summarised in Table 6 based on an hourly hydrogen production rate of 49 kg. The GHG impact of the CLH2 process under consideration is 18,690 $gCO_2e/kg\ H_2$ produced or 154 $gCO_2e/MJ\ H_2$. The impact is dominated by the need to supply process heat to the fuel reactor(redox heater emissions:9,628 $gCO_2/kg\ H_2$) as shown in Figure 8.

Inputs	Value	Units	Comments
Resources			
Natural gas	99	kg	Natural gas for reaction
Oxide material	1.26	kg	Yearly make-up (per hour)
Water	440	kg	Make-up water (reaction and cooling)
Energy			
Natural gas	151	kg	Fuel reactor heat requirement
Electricity	189	kW	Net electricity requirement
Outputs			
Hydrogen	49	kg	Compressed hydrogen output
Emissions			
H_2O	217	kg	Fuel reactor (stack emissions)
CO_2	272	kg	Fuel reactor (stack emissions)
CO_2	419	kg	Fuel reactor (heater emissions)

Table 6. LCA inputs/outputs (per hour) for the CLH2 process.

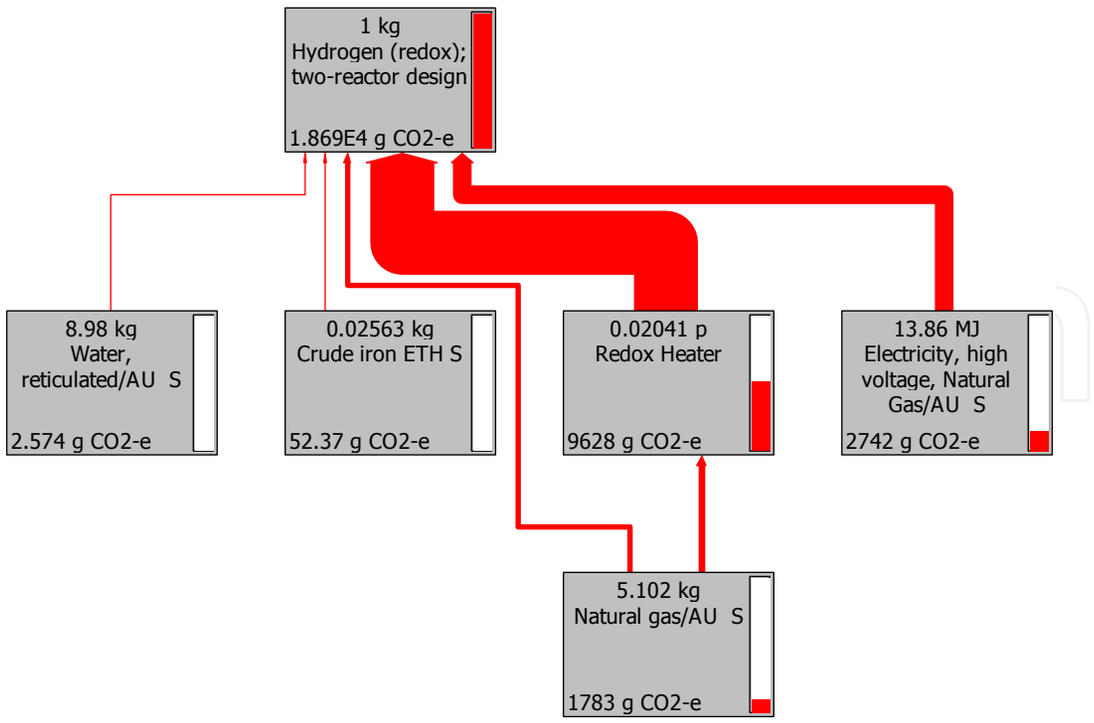

Emissions source	g $CO_2e/kg\ H_2$
Direct redox reaction emissions	5,558.6
Water supply	2.6
Gas supply (reaction feedstock)	706.1
Oxide material	52.4
Fuel reactor (process heat)	9,628.0
Electricity (from natural gas)	2,742.0
Total	18,689.7

Figure 8. Redox emissions breakdown (per kg H_2).

Preliminary results demonstrate the need to optimise the delivery of heat to the fuel reactor. The introduction of a third combustion loop operated at higher temperature is one such means to reduce upstream emissions. However, this may negatively influence total capital expenditure. The literature reports hydrogen production through current steam reforming technology produces between 9,830 $gCO_2e/kg\ H_2$ (24,000 kg H_2/day; midsized facility) and 12,130 $gCO_2e/kg\ H_2$ (480 kg H_2/day; distributed facility), and thus are higher than the direct redox process emissions [56], although significantly lower than the total CLH2 emissions. The literature only considered electricity and natural gas related emissions and thus total upstream emissions of existing technologies maybe higher than the reported values.

The commercial viability of the redox process was estimated using cost estimate practices outlined in the literature [56, 57]. Results are reported in \$/kg H_2. Material and fuel operating expenditure was calculated using the inputs identified in Figure7, as summarised in the lifecycle analysis section (Table 6). Fixed operating and maintenance costs were

calculated based on the total capital expenditure. Battery limit capital expenditure (e.g. redox process) is based on the engineering judgment of the authors, with capital build-up (facilities, engineering, permitting, start-up, contingencies, working capital and land) estimated using a percentage of the battery limit cost. Capital charges are calculated using a percentage of total capital expenses. Importantly, although the estimates may look precise, they are simply estimates based on the judgment of the authors. There remains significant uncertainty about the actual cost of the redox process as it has not been commercially demonstrated. A breakdown of cost data is provided in Table 7.

Initial costing estimates show that the redox process may produce hydrogen at $8.93/kg ($9.36/kg, including carbon tax). The cost breakdown demonstrates that onsite storage of compressed hydrogen represents a significant expense. However, this arises from the conversion of stranded methane. If demand for hydrogen is identified close to a stranded gas reserve, storage costs will decrease significantly. Delivery of compressed hydrogen represents an additional cost that has not been considered in this analysis. Literature cost estimates for at

Expense	$M/yr	Comment
OpEX		Variable (fuel and materials)
Oxide material	0.55	$50/kg
Natural gas	0.20	Reaction feed and reducer heating
Electricity	0.12	Net electricity demand
Water	0.01	Make-up supply
Total OpEX	**0.88**	
CapEX	**$M**	
CLH2 reactor	10.0	
H_2 Compression	0.44	$3,000/kW capacity
H_2 Storage	5.97	$26,417/$m^3$ capacity; 5 days storage
Total process units	16.42	
General facilities	3.28	20 % of process unit CapEX
Engineering	2.46	15 % of process unit CapEX
Contingencies	1.64	10 % of process unit CapEX
Working capital	0.82	5 % of process unit CapEX
Total CapEX	24.62	
Balance	**$M/yr**	
OpEx (variable)	0.88	
OpEx (fixed)	0.49	2 % of total CapEX
Capital charge	2.46	10 % of total CapEX
Carbon Tax	0.18	$23/T CO_2
Total ($M/yr)	**4.02**	
Total ($/kg H_2)	**8.93**	**(ex. carbon tax)**
	9.36	**(inc. carbon tax)**

Table 7. Redox process cost estimates.

gate hydrogen production via steam reforming, using current technology, range between $1.51/kg (midsize facility: 24,000 kg H_2/day) to $3.68/kg (distributed facility: 480 kg H_2/day facility). Hence the hydrogen at gate cost for the CLH2 process is higher than steam reforming technology. Electrolysis production of hydrogen ranges between $4.94 and $6.82 per kg for a midsize and distributed facility respectively and thus is closer to CLH2production costs [56]. Experience gained through the commercialisation and deployment of the redox technology is expected to reduce costs, particularly capital build-up costs. However the stranded nature of the product may significantly increase total delivered hydrogen cost.

5. Conclusion

The feasibility of producing hydrogen from the metal/metal oxide redox process has been demonstrated in the literature. This process offers several advantages including the ability to produce hydrogen of high purity and a concentrated stream of carbon dioxide. Most importantly this process eliminates the need for a supply of high purity oxygen and a water gas shift process that are generally required by commercial processes. However, this redox process is not regarded as a fully developed technology and further R&D development is required for commercialisation.

In view of the literature, much research effort has been devoted to formulating novel oxygen carrier materials. Although several types of improved oxygen carrier materials have been identified, full appraisals of their performance and further optimisation studies are required. Iron oxides and nickel oxides appear to be attractive candidates for this application in terms of their activity. However, their thermal stabilities need further improvement. Current practices include doping, introducing a diffusional barrier provided by a second oxide, and/or adding a second oxide with higher oxygen storage capacity. There are also a limited number of studies that investigate the life time of oxygen carriers. Apart from chemical stability, the changes in the physical properties such as size and attrition of the carrier particles during fluidisation have received little attention and should be addressed in future research. It is viewed strongly that improvement in these areas would significantly increase process efficiency and economic viability of the cyclic redox process.

The lack of pilot scale studies also impedes the commercialisation of cyclic redox and chemical looping processes. Limited data are available for process design, scale-up and optimisation. For example, the transfer of the oxygen carrier particles between oxidation and reduction is a critical issue when it comes to process design. Fixed bed, moving bed and circulating fluidised bed have been proposed, and the choice of reactor will depend on the reaction kinetics and the required flow dynamics of the process. Because the cyclic redox process is considered as an unsteady process, the definition of the operation window of the process will be determined by limiting the upper and the lower oxidation states of the metal/metal oxide couple. This parameter has a direct impact on the overall conversion efficiencies, process designs and economics. Since the redox reactions usually take place at temperatures above 600 °C, most of the sensible heat stored in the gas existing from the oxidation and reduction reactors can be used to generate power with a steam generator. The co-production of excess electricity would reduce the cost of the hydrogen produced and

increase overall process viability. Hence, the issue of heat management requires much closer examination when it comes to process optimisation.

Finally, the current preliminary LCA-Economic study has made the first attempt to provide an indicative price of hydrogen produced from the redox process. Although the cost of hydrogen produced from the redox process is higher than hydrogen produced from other commercial processes, several design parameters have been identified as the areas for future improvement. It is seen that the LCA techniques are valuable tools for process optimisation.

Author details

Doki Yamaguchi, Liangguang Tang, Nick Burke and Ken Chiang*
CSIRO Earth Science and Resource Engineering, Australia

Lucas Rye
CSIRO Marine and Atmospheric Research, Australia

Trevor Hadley and Seng Lim
CSIRO Process Science and Engineering, Australia

Acknowledgement

The authors acknowledge the support from CSIRO Petroleum and Geothermal Research Portfolio in conducting this study

6. References

[1] IEA (2005) Prospects for Hydrogen and Fuel Cells. OECD Publishing
[2] Mueller-Langer, F., Tzimas, E., Kaltschmitt, M., and Peteves, S. (2007) Techno-economic assessment of hydrogen production processes for the hydrogen economy for the short and medium term. Int. J. Hydrogen Energy 32: 3797-3810.
[3] Pardro, C.E.G. and Putsche, V., Survey of the Economics of Hydrogen Technologies. 1999, National Renewable Energy Laboratory: Golden, Colorado.
[4] Mirabal, S.T., (2003) An Economic Analysis of Hydrogen Production Technologies Using Renewable Energy Resources, University of Florida.
[5] Raissi, A.T. and Block, D.L. (2004) Hydrogen - automotive fuel of the future. IEEE Power Energ. Mag. November/December 40-45.
[6] Fan, L.S. and Li, F.X. (2010) Chemical Looping Technology and Its Fossil Energy Conversion Applications. Ind. Eng. Chem. Res. 49: 10200-10211.
[7] Adanez, J., Abad, A., Garcia-Labiano, F., Gayan, P., and de Diego, L.F. (2012) Progress in Chemical-Looping Combustion and Reforming technologies. Prog. Energy Combust. Sci. 38: 215-282.
[8] Gupta, P., Velazquez-Vargas, L.G., and Fan, L.S. (2007) Syngas redox (SGR) process to produce hydrogen from coal derived syngas. Energy Fuels 21: 2900-2908.

* Corresponding Author

[9] Li, F., Kim, H.R., Sridhar, D., Wang, F., Zeng, L., Chen, J., and Fan, L.S. (2009) Syngas Chemical Looping Gasification Process: Oxygen Carrier Particle Selection and Performance. Energy Fuels 23: 4182-4189.
[10] Li, F.X., Zeng, L., Velazquez-Vargas, L.G., Yoscovits, Z., and Fan, L.S. (2010) Syngas Chemical Looping Gasification Process: Bench-Scale Studies and Reactor Simulations. AlChE J. 56: 2186-2199.
[11] Yang, J.B., Cai, N.S., and Li, Z.S. (2008) Hydrogen production from the steam-iron process with direct reduction of iron oxide by chemical looping combustion of coal char. Energy Fuels 22: 2570-2579.
[12] Fan, L., Li, F., and Ramkumar, S. (2008) Utilization of chemical looping strategy in coal gasification processes. Particuology 6: 131-142.
[13] Gnanapragasam, N.V., Reddy, B.V., and Rosen, M.A. (2009) Hydrogen production from coal using coal direct chemical looping and syngas chemical looping combustion systems: Assessment of system operation and resource requirements. Int. J. Hydrogen Energy 34: 2606-2615.
[14] Sime, R., Kuehni, J., D'Souza, L., Elizondo, E., and Biollaz, S. (2003) The redox process for producing hydrogen from woody biomass. Int. J. Hydrogen Energy 28: 491-498.
[15] Kobayashi, N. and Fan, L.S. (2010) Biomass direct chemical looping process: A perspective. Biomass Bioenergy 35: 1252-1262.
[16] Li, F.X., Zeng, L., and Fan, L.S. (2010) Biomass direct chemical looping process: Process simulation. Fuel 89: 3773-3784.
[17] Hacker, V., Faleschini, G., Fuchs, H., Fankhauser, R., Simader, G., Ghaemi, M., Spreitz, B., and Friedrich, K. (1998) Usage of biomass gas for fuel cells by the SIR process. J. Power Sources 71: 226-230.
[18] Bleeker, M.F., Kersten, S.R.A., and Veringa, H.J. (2007) Pure hydrogen from pyrolysis oil using the steam-iron process. Catal. Today 127: 278-290.
[19] Bleeker, M.F., Veringa, H.J., and Kersten, S.R.A. (2010) Pure Hydrogen Production from Pyrolysis Oil Using the Steam-Iron Process: Effects of Temperature and Iron Oxide Conversion in the Reduction. Ind. Eng. Chem. Res. 49: 53-64.
[20] Galvita, V.V., Poelman, H., and Marin, G.B. (2011) Hydrogen Production from Methane and Carbon Dioxide by Catalyst-Assisted Chemical Looping, . Top. Catal. 54 907-913.
[21] Cormos, C.-C. (2011) Hydrogen production from fossil fuels with carbon capture and storage based on chemical looping systems. Int. J. Hydrogen Energy 36: 5960-5971.
[22] Otsuka, K., Kaburagi, T., Yamada, C., and Takenaka, S. (2003) Chemical storage of hydrogen by modified iron oxides. J. Power Sources 122: 111-121.
[23] Otsuka, K., Yamada, C., Kaburagi, T., and Takenaka, S. (2003) Hydrogen storage and production by redox of iron oxide for polymer electrolyte fuel cell vehicles. Int. J. Hydrogen Energy 28: 335-342.
[24] Wang, H., Wang, G., Wang, X., and Bai, J. (2008) Hydrogen production by redox of cation-modified iron oxide. J. Phys. Chem. C 112: 5679-5688.
[25] Liu, X. and Wang, H. (2010) Hydrogen production from water decomposition by redox of Fe_2O_3 modified with single- or double-metal additives. J. Solid State Chem. 183: 1075-1082.
[26] Otsuka, K. and Takenaka, S. (2004) Storage and supply of pure hydrogen mediated by the redox of iron oxides. J. Jpn. Pet. Inst. 47: 377-386.

[27] Ryu, J.C., Lee, D.H., Kang, K.S., Park, C.S., Kim, J.W., and Kim, Y.H. (2008) Effect of additives on redox behavior of iron oxide for chemical hydrogen storage. J. Ind. Eng. Chem. 14: 252-260.
[28] Kodama, T., Watanabe, Y., Miura, S., Sato, M., and Kitayama, Y. (1996) Reactive and selective redox system of Ni(II)-ferrite for a two-step CO and H_2 production cycle from carbon and water. Energy 21: 1147-1156.
[29] Kang, K.S., Kim, C.H., Cho, W.C., Bae, K.K., Woo, S.W., and Park, C.S. (2008) Reduction characteristics of $CuFe_2O_4$ and Fe_3O_4 by methane; $CuFe_2O_4$ as an oxidant for two-step thermochemical methane reforming. Int. J. Hydrogen Energy 33: 4560-4568.
[30] Takenaka, S., Hanaizumi, N., Son, V.T.D., and Otsuka, K. (2004) Production of pure hydrogen from methane mediated by the redox of Ni- and Cr-added iron oxides. J. Catal. 228: 405-416.
[31] Urasaki, K., Tanimoto, N., Hayashi, T., Sekine, Y., Kikuchi, E., and Matsukata, M. (2005) Hydrogen production via steam-iron reaction using iron oxide modified with very small amounts of palladium and zirconia. Appl. Catal., A 288: 143-148.
[32] Adanez, J., de Diego, L.F., Garcia-Labiano, F., Gayan, P., Abad, A., and Palacios, J.M. (2004) Selection of Oxygen Carriers for Chemical-looping Combustion. Energy Fuels 18: 371-377.
[33] Cho, P., Mattisson, T., and Lyngfelt, A. (2004) Comparison of iron-, nickel-, copper- and manganese-based oxygen carriers for chemical-looping combustion. Fuel 83: 1215-1225.
[34] Zafar, Q., Mattisson, T., and Gevert, B. (2005) Integrated hydrogen and power production with CO_2 capture using chemical-looping reforming-redox reactivity of particles of CuO, Mn_2O_3, NiO, and Fe_2O_3 using SiO_2 as a support. Ind. Eng. Chem. Res. 44: 3485-3496.
[35] Kodama, T., Shimizu, T., Satoh, T., Nakata, M., and Shimizu, K.I. (2002) Stepwise production of CO-RICH syngas and hydrogen via solar methane reforming by using a Ni(II)-ferrite redox system. Sol. Energy 73: 363-374.
[36] Kodama, T., Kondoh, Y., Yamamoto, R., Andou, H., and Satou, N. (2005) Thermochemical hydrogen production by a redox system of ZrO_2-supported Co(II)-ferrite. Sol. Energy 78: 623-631.
[37] Cha, K.S., Yoo, B.K., Kim, H.S., Ryu, T.G., Kang, K.S., Park, C.S., and Kim, Y.H. (2010) A study on improving reactivity of Cu-ferrite/ZrO_2 medium for syngas and hydrogen production from two-step thermochemical methane reforming. Int. J. Energy Res. 34: 422-430.
[38] Kang, K.S., Kim, C.H., Bae, K.K., Cho, W.C., Kim, S.H., Kim, W.J., Kim, Y.H., and Park, C.S. (2010) Redox cycling of $CuFe_2O_4$ supported on ZrO_2 and CeO_2 for two-step methane reforming/water splitting. Int. J. Hydrogen Energy 35: 568-576.
[39] Li, K.Z., Wang, H., Wei, Y.G., and Yan, D.X. (2009) Selective Oxidation of Carbon Using Iron-Modified Cerium Oxide. J. Phys. Chem. C 113: 15288-15297.
[40] Tang, L., Yamaguchi, D., Burke, N., Trimm, D., and Chiang, K. (2010) Methane decomposition over ceria modified iron catalysts. Catal. Commun. 11: 1215-1219.
[41] Yamaguchi, D., Tang, L., Wong, L., Burke, N., Trimm, D., Nguyen, K., and Chiang, K. (2011) Hydrogen production through methane-steam cyclic redox processes with iron-based metal oxides. Int. J. Hydrogen Energy 36: 6646-6656.

[42] Sim, A., Cant, N.W., and Trimm, D.L. (2010) Ceria-zirconia stabilised tungsten oxides for the production of hydrogen by the methane-water redox cycle. Int. J. Hydrogen Energy 35: 8953-8961.
[43] Galvita, V. and Sundmacher, K. (2005) Hydrogen production from methane by steam reforming in a periodically operated two-layer catalytic reactor. Appl. Catal., A 289: 121-127.
[44] Datta, P., Rihko-Struckmann, L.K., and Sundmacher, K. (2011) Influence of molybdenum on the stability of iron oxide materials for hydrogen production with cyclic water gas shift process. Mater. Chem. Phys. 129: 1089-1095.
[45] Leion, H., Mattisson, T., and Lyngfelt, A. (2009) Use of Ores and Industrial Products As Oxygen Carriers in Chemical-Looping Combustion. Energy Fuels 23: 2307-2315.
[46] Leion, H., Lyngfelt, A., Johansson, M., Jerndal, E., and Mattisson, T. (2008) The use of ilmenite as an oxygen carrier in chemical-looping combustion. Chem. Eng. Res. Des 86: 1017-1026.
[47] Adanez, J., Cuadrat, A., Abad, A., Gayan, P., de Diego, L.F., and Garcia-Labiano, F. (2010) Ilmenite Activation during Consecutive Redox Cycles in Chemical-Looping Combustion. Energy Fuels 24: 1402-1413.
[48] Leion, H., Mattisson, T., and Lyngfelt, A. (2008) Solid fuels in chemical-looping combustion. Int. J. Greenhouse Gas Control 2: 180-193.
[49] Lorente, E., Pena, J.A., and Herguido, J. (2011) Cycle behaviour of iron ores in the steam-iron process. Int. J. Hydrogen Energy 36: 7043-7050.
[50] Fukase, S. and Suzuka, T. (1993) Residual oil cracking with generation of hydrogen - Deactivation of iron-oxide catalyst in the steam iron reaction. Appl. Catal., A 100: 1-17.
[51] Cho, P., Mattisson, T., and Lyngfelt, A. (2005) Carbon formation on nickel and iron oxide-containing oxygen carriers for chemical-looping combustion. Ind. Eng. Chem. Res. 44: 668-676.
[52] Hadley, T.D., Chiang, K., Burke, N.R., and Lim, K.S. (2010) Multiple-loop chemical reactor design with pressure balance consideration. Fluidization XIII 463-470.
[53] ISO, ISO/DIS14040, Environmental Management Standard - Life Cycle Assessment, Principlesand Framework. International Standard. Switzerland. 2006.
[54] Horne, R., Grant, T., and Verghese, K. (2009) Life Cycle Assessment: Principles, Practice and Prospects. CSIRO
[55] Weidema, B.P., Rebitzer, G., and Ekvall, T. (2004) Scenarios in Life-cycle Assessment Society of Environmental Toxicology and Chemistry
[56] NRC (2004) The Hydrogen Economy: Opportunities, Costs, Barriers, and R&D Needs. The National Academies Press.
[57] Simbeck, D. and Chang, E. (2002) Hydrogen Supply: Cost Estimate for Hydrogen Pathways Scoping Analysis . NREL, Report: SR-540-3252. National Renewable Energy Laboratory